Downloaded from orbit.dtu.dk on: Mar 27, 2023

DTU Library

# Hall effect measurement for precise sheet resistance and thickness evaluation of Ruthenium thin films using non-equidistant four-point probes

**Østerberg, Frederik Westergaard; Witthøft, Maria-Louise; Dutta, Shibesh; Meersschaut, Johan; Adelmann, Christoph; Nielsen, Peter Folmer; Hansen, Ole; Petersen, Dirch Hjorth**

*Published in:*
A I P Advances

*Link to article, DOI:*
10.1063/1.5010399

*Publication date:*
2018

*Document Version*
Publisher's PDF, also known as Version of record

Link back to DTU Orbit

*Citation (APA):*
Østerberg, F. W., Witthøft, M-L., Dutta, S., Meersschaut, J., Adelmann, C., Nielsen, P. F., Hansen, O., & Petersen, D. H. (2018). Hall effect measurement for precise sheet resistance and thickness evaluation of Ruthenium thin films using non-equidistant four-point probes. *A I P Advances*, *8*(5), [055206]. https://doi.org/10.1063/1.5010399

**General rights**
Copyright and moral rights for the publications made accessible in the public portal are retained by the authors and/or other copyright owners and it is a condition of accessing publications that users recognise and abide by the legal requirements associated with these rights.

- Users may download and print one copy of any publication from the public portal for the purpose of private study or research.
- You may not further distribute the material or use it for any profit-making activity or commercial gain
- You may freely distribute the URL identifying the publication in the public portal

If you believe that this document breaches copyright please contact us providing details, and we will remove access to the work immediately and investigate your claim.

**Hall effect measurement for precise sheet resistance and thickness evaluation of Ruthenium thin films using non-equidistant four-point probes**

Frederik Westergaard Østerberg, Maria-Louise Witthøft, Shibesh Dutta, Johan Meersschaut, Christoph Adelmann, Peter Folmer Nielsen, Ole Hansen, and Dirch Hjorth Petersen

Citation: AIP Advances **8**, 055206 (2018); doi: 10.1063/1.5010399
View online: https://doi.org/10.1063/1.5010399
View Table of Contents: http://aip.scitation.org/toc/adv/8/5
Published by the American Institute of Physics

PHYSICS TODAY
WHITEPAPERS
MANAGER'S GUIDE
Accelerate R&D with Multiphysics Simulation
READ NOW
PRESENTED BY

AIP ADVANCES **8**, 055206 (2018)

# Hall effect measurement for precise sheet resistance and thickness evaluation of Ruthenium thin films using non-equidistant four-point probes

Frederik Westergaard Østerberg,[1,2] Maria-Louise Witthøft,[1] Shibesh Dutta,[3,4,a] Johan Meersschaut,[3] Christoph Adelmann,[3] Peter Folmer Nielsen,[2] Ole Hansen,[1] and Dirch Hjorth Petersen[1,b]

[1] *DTU Nanotech - Department of Micro- and Nanotechnology, Technical University of Denmark, Building 345 East, DK-2800 Kongens Lyngby, Denmark*
[2] *CAPRES A/S, Scion-DTU, Building 373, DK-2800 Kongens Lyngby, Denmark*
[3] *Imec, Kapeldreef 75, 3001 Leuven, Belgium*
[4] *KU Leuven, Department of Physics and Astronomy, Celestijnenlaan 200d, 3001 Leuven, Belgium*

(Received 25 October 2017; accepted 25 April 2018; published online 8 May 2018)

We present a new micro Hall effect measurement method using non-equidistant electrodes. We show theoretically and verify experimentally that it is advantageous to use non-equidistant electrodes for samples with low Hall sheet resistance. We demonstrate the new method by experiments where Hall sheet carrier densities and Hall mobilities of Ruthenium thin films (3-30 nm) are determined. The measurements show that it is possible to measure Hall mobilities as low as 1 $cm^2V^{-1}s^{-1}$ with a relative standard deviation of 2-3%. We show a linear relation between measured Hall sheet carrier density and film thickness. Thus, the method can be used to monitor thickness variations of ultra-thin metal films. © *2018 Author(s). All article content, except where otherwise noted, is licensed under a Creative Commons Attribution (CC BY) license (http://creativecommons.org/licenses/by/4.0/).* https://doi.org/10.1063/1.5010399

## I. INTRODUCTION

Since the invention of the integrated circuit, microelectronics technology has developed at a break-neck speed to the current level, where extremely sophisticated, highly complex systems can be squeezed into minute microelectronic chips with a functionality that affects our every-day life. This development has been supported not only by groundbreaking developments in fabrication technology and ingenuous circuit design but also by significant advances in metrology. Metrology is increasingly important in production for process control, in research to support development of new technology, and in science to understand limitations and opportunities imposed by small size effects, which may eventually slow down the speed of new technology developments in the microelectronics industry.

A key metrology task is the characterization of the electronic transport properties of thin films of semiconductors and metals,[1] to provide direct measurements of sheet resistance, sheet carrier density and carrier mobility; key parameters for the functionality and performance of microelectronic devices. Traditionally, sheet resistance measurements have been done using macroscopic four-point probes,[1,2] however, the development of the micro four-point probe,[3,4] which offers significant advantages compared to macroscopic probes, has created new metrology opportunities for characterizing transport properties of materials.[5]

Sheet carrier density and carrier mobility can be extracted from Hall effect measurements,[1] which traditionally are done on structured samples such as cloverleafs or small squares in van der Pauw configuration.[6] The traditional methods can be used to measure mobilities well below

[a] Current affiliation: Advanced Process Development - Singapore, Micron Technology Inc., Fab10N Singapore, 757432.
[b] Electronic mail: Dirch.Petersen@nanotech.dtu.dk

 © Author(s) 2018

1 cm$^2$/(Vs).[6] The traditional methods, however, require significant sample preparation, e.g., a sample piece must be cut out and contacts deposited on the corners of the sample. The micro Hall effect method has been demonstrated as a powerful alternative.[7] Here a micro four-point probe is positioned on a thin film sample in proximity of an electrically insulating boundary. Hall effect measurements are then performed with a constant magnetic flux density ($B_z$) perpendicular to the sample surface. Each measurement takes just 10 s, and as a result this method is particularly convenient in process development and for process control. The direct result of the micro Hall effect measurement is the sheet resistance ($R_0$) and the Hall sheet resistance ($R_{\mathrm{H}}$) from which the Hall mobility ($\mu_{\mathrm{H}}$) and the Hall sheet density ($N_{\mathrm{HS}}$) can be calculated.

The micro Hall effect method was developed for four-point probes with equidistant electrodes.[7] However, here we show, theoretically, that it is advantageous to use a probe with non-equidistant electrodes, in agreement with other geometry dependent studies where precision is improved by optimizing electrode distances.[8–10] We verify the theoretical prediction in a series of measurements on thin Ruthenium films (3-30 nm) where sheet resistance, Hall sheet resistance, Hall mobility and Hall sheet carrier density are determined.

A key element in extracting Hall effect information from the four-point probe measurement is determination of the distance ($y_0$) from the probe to the insulating straight boundary, and thus the procedure after the four-point probe measurements can be separated into two steps; 1) extraction of the probe-boundary distance $y_0$ and the sheet resistance $R_0$; 2) extraction of the Hall sheet resistance ($R_{\mathrm{H}}$) based on the probe position from step 1). From $R_0$ and $R_{\mathrm{H}}$ the Hall mobility and Hall sheet carrier density can be calculated using[7]

$$\mu_{\mathrm{H}} = \frac{R_{\mathrm{H}}}{R_0 Z B_z}, \quad N_{\mathrm{HS}} = \frac{Z B_z}{e R_{\mathrm{H}}}, \tag{1}$$

where $Z$ is the carrier type ($Z = \pm 1$) and $e$ is the unit charge.

Previously, multiple methods for determining the distance $y_0$ have been demonstrated. The distance $y_0$ can be found by fitting a model to a series of measurements recorded at different distances to the boundary, where the distances between measurement positions are known.[7] It has also been shown that it is possible to use only two measurement positions, that can be either far apart[11] or closely spaced.[12] A particularly convenient single engage method to determine $y_0$ using two four-point sub-probes (with different pitch) of a 7 point probe has also been developed.[13]

However, for many samples determining the distance between the probe and the insulating boundary is not the main source of error. The main source of error is often dependent on how accurately $R_{\mathrm{H}}$ can be determined. This is especially true for thin film metal samples where $R_{\mathrm{H}} \ll R_0$.

In this study we focus on methods to reduce the effects of the noise sources affecting $R_{\mathrm{H}}$. The study will only use the single engage method of determining $y_0$ but the findings may be applied the the other methods as well. Instead of being limited to using only equidistant four-point probes, we will investigate how the precision will be affected by using non-equidistant four-point probes to determine the Hall sheet resistance.

## II. THEORY

For this study a 7 point probe with equidistant electrode spacings will be used like the ones shown in Fig. 1. For each measurement only 4 electrodes are used, two for passing a current through the sample and two for measuring a voltage. A set of 4 of the 7 electrodes is called a sub-probe. The sub-probe sketched in Fig. 1 uses pins 1,3,5 and 7 and will for simplicity be called sub-probe 1357. Figure 1 also shows how the electrode pitches $a$, $b$ and $c$ of a sub-probe are defined, $a$ is the distance between the first and second electrode used, $b$ is the distance between the second and third electrodes and $c$ is the distance between third and forth electrodes. The electrode configurations B and B' shown in Fig. 1 are the ones commonly used for Hall measurements to determine $R_{\mathrm{H}}$. The A and A' configurations are used only when determining $y_0$ and $R_0$ and are therefore not illustrated.

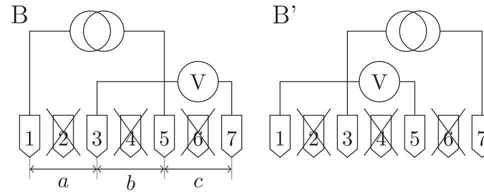


FIG. 1. Arrangement of current and voltage electrodes for B and B' probe configurations. The sub-probe depicted is called 1357 because of the electrodes used. Definitions of the electrode spacings $a$, $b$ and $c$ are also shown.

When the probe is placed parallel to the insulating boundary at a distance ($y_0$) and a current ($I_0$) is passed through the sample, the theoretical average resistance in the B and B' configuration is

$$\begin{aligned}\overline{R_{BB'}} &= (V_B + V_{B'})/(2I_0)\\ &= \mathcal{A}_+ \ln \frac{b(a+b+c)}{ac} + \mathcal{A}_- \ln \sqrt{\frac{(b^2+4y_0^2)((a+b+c)^2+4y_0^2)}{(a^2+4y_0^2)(c^2+4y_0^2)}},\end{aligned} \tag{2}$$

where

$$\mathcal{A}_+ \equiv \frac{R_0}{2\pi}\left(1+\frac{R_H^2}{R_0^2}\right), \quad \mathcal{A}_- \equiv \frac{R_0}{2\pi}\left(1-\frac{R_H^2}{R_0^2}\right). \tag{3}$$

Similarly, the theoretical difference between the resistances in the B and B' configurations is

$$\begin{aligned}\Delta R_{BB(')} &= (V_B - V_{B'})/(I_0)\\ &= \frac{2R_H}{\pi}\left(\arctan\frac{a}{2y_0} + \arctan\frac{b}{2y_0} + \arctan\frac{c}{2y_0} - \arctan\frac{a+b+c}{2y_0}\right).\end{aligned} \tag{4}$$

Equation (2) shows that the average resistance $\overline{R_{BB'}}$ only consists of the log terms and is proportional to $R_0$ for $R_H \ll R_0$. Likewise, the resistance difference $\Delta R_{BB'}$ consists only of arctan terms and is proportional to $R_H$.

When determining $\Delta R_{BB'}$ the two main sources of error are electrode position error and electrical noise. The electrode position error arises from the fact that the electrode will not land at their nominal position. The electrical noise arises from the signal to noise ratio of measurement electronics.

The position error can be quantified by calculating the sensitivity of $\Delta R_{BB'}$ to the movement of each electrode. This sensitivity is found by calculating the partial derivatives $\partial\Delta R_{BB'}/\partial x_i$, where $x_i$ is the position of the $i$'th electrode. Any position error due to movements of electrode 1 or 4 will effectively result in a change of width, which will be compensated for when the distance to the insulating boundary is calculated. Thus, only position errors related to electrode 2 and 3 are of interest. By using that $x_2 - x_1 = a$, $x_3 - x_2 = b$, $x_4 - x_3 = c$ the sensitivities for electrode 2 and 3 can be calculated as

$$\frac{\partial\Delta R_{BB'}}{\partial x_2} = \frac{4R_H y_0}{\pi}\frac{b^2-a^2}{(a^2+4y_0^2)(b^2+4y_0^2)} \tag{5}$$

$$\frac{\partial\Delta R_{BB'}}{\partial x_3} = \frac{4R_H y_0}{\pi}\frac{c^2-b^2}{(b^2+4y_0^2)(c^2+4y_0^2)} \tag{6}$$

These equations show that for an equidistant four-point probe ($a = b = c$) the sensitivity to movement of electrode 2 and 3 becomes 0.

From the partial derivatives the relative standard deviation ($\sigma_{rel}$) of $\Delta R_{BB'}$ can be estimated by

$$\sigma_{rel}(\Delta R_{BB'}) = \frac{\sigma_x}{\Delta R_{BB'}}\sqrt{\sum_{i=2}^{3}\left(\frac{\partial\Delta R_{BB'}}{\partial x_i}\right)^2}, \tag{7}$$

where $\sigma_x$ is the standard deviation of the position error for each electrode (the standard deviation is assumed identical for all electrodes).

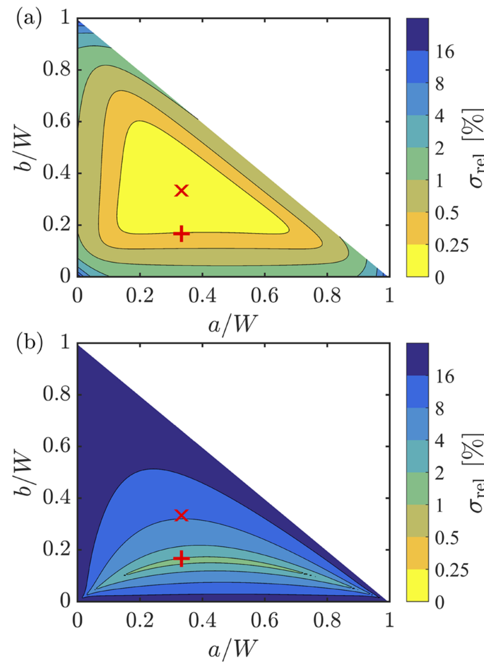


FIG. 2. Relative standard deviation of $\Delta R_{BB'}$ due to position errors (a) and due to electrical noise (b) as function of $a/W$ and $b/W$. The plots were calculated using the following settings: $y_0/W = 4/60$, $\sigma_x/W = 0.1/60$, $R_0/R_H = 5000$, SNR = 10000, $R_{min} = 30\ \mu\Omega$. The symbol × corresponds to an equidistant probe ($a = b = c = W/3$) and the symbol + corresponds to the non-equidistant probe $a = W/3$, $b = W/6$ and $c = W/2$.

In Fig. 2(a) the relative standard deviation of $\Delta R_{BB'}$ is plotted as function of $a$ and $b$ normalized with the probe width ($W = a + b + c$). The plot is calculated for the following settings $y_0/W = 4/60$ and $\sigma_x/W = 0.1/60$. The symbol × corresponds to an equidistant probe ($a = b = c = W/3$) and the symbol + corresponds to the non-equidistant probe $a = W/3$, $b = W/6$ and $c = W/2$. Figure 2(a) shows that the smallest relative error is obtained for the equidistant probe.

The other important source of error is the electrical noise. The electrical noise is composed of two terms; a part related to the signal to noise ratio (SNR) of the measurement and a part related to the minimum possible resistance the electronics can resolve ($R_{min}$). Since $\Delta R_{BB'}$ is the difference between 2 measurement configurations repeated $N$ times the relative standard deviation of $\Delta R_{BB'}$ for electrical noise will have a prefactor of $\sqrt{2/N}$. Each measurement will have a standard error of $\overline{R_{BB'}}/\mathrm{SNR} + R_{min}$. Thus it is possible to estimate the relative standard deviation of $\Delta R_{BB'}$ from

$$\sigma_{rel}(\Delta R_{BB'}) = \frac{\sqrt{\frac{2}{N}}\left(\frac{\overline{R_{BB'}}}{\mathrm{SNR}} + R_{min}\right)}{\Delta R_{BB'}}. \tag{8}$$

From experiments, similar to those of Kjaer et al.,[14] we have found that SNR=10000 and the minimum resistance ($R_{min}$) that can be resolved in a single measurement is roughly 30 $\mu\Omega$. In Fig. 2(b), the relative standard deviation of $\Delta R_{BB'}$ due to electrical noise is plotted as function of $a$ and $b$. For the plot, the following parameters were used: $R_0$=5 Ω, $R_0/R_H = 5000$, $y_0/W = 4/60$. This plot shows that the lowest relative standard deviation is obtained for the non-equidistant probe.

## III. EXPERIMENTAL

In order to determine experimentally which sub-probe yields the lowest standard deviation for Hall measurements a series of measurements were performed on Ruthenium (Ru) thin film samples of varying thicknesses (3-30 nm). All samples were prepared by atomic layer deposition of Ru on

TiN (0.3 nm)/$SiO_2$ (90 nm)/Si, as described by Wen et al.[15] and Popovici et al.[16] The Ru area density $N_{RBS}$ of the samples was measured by Rutherford backscattering spectrometry (RBS).[17] The Ru film thickness $d$ was calculated from $N_{RBS}$ assuming a bulk Ru density of $n_{Ru} \simeq 7.4 \times 10^{22}$ cm$^{-3}$, i.e., $d = N_{RBS}/n_{Ru}$. Prior to the M4PP measurements the samples were cleaved in order to get straight insulating boundaries to perform Hall measurements at.

The measurements were performed using a microHall-M300 tool from CAPRES A/S and a micro 7-point probe (M7PP) with all electrode distances fixed at 10 $\mu$m. A magnetic field with the flux density $B_z$ = 600 mT was applied perpendicular to the sample. The probe was placed nominally 4 $\mu$m from the insulating boundary during measurements. For each sample, 7 engages were performed parallel to the insulating boundary, thus keeping the distance between the probe and insulating boundary constant. At each point of the linescan A, A', B and B' configurations were measured for sub-probes 1234, 4567 and 1357 in order to be able to determine the distance to the edge and the sheet resistance of the sample. The reason both sub-probes 1234 and 4567 were recorded was to be able to eliminate any small rotational misalignments between the probe and the insulating boundary. Furthermore, during the same engage, 6 B and 6 B' configurations were measured using both sub-probes 1357 (equidistant) and 1347 (non-equidistant) in order to determine the Hall sheet resistance.

## IV. RESULTS & DISCUSSION

From the measurements $R_0$ and $R_H$ were determined and in Fig. 3(a) the results are plotted as function of sample thickness; the error bars correspond to one standard deviation. In order to relate the measured $R_0$ and $R_H$ to resistivities the resistance values were multiplied with sample thickness.

From $R_0$ and $R_H$ the Hall mobility $\mu_H$ and the Hall sheet carrier density $N_{HS}$ can be calculated from Eq. 1. The calculated values of the $N_{HS}$ and $\mu_H$ are plotted as function of sample thickness in Fig. 3(b), where the error bars correspond to one standard deviation. The blue dashed line through the Hall sheet carrier density points is the corresponding linear fit. The Hall sheet carrier density is expected to be proportional to the sample thickness, but from the linear fit it is seen that there is an offset, which could suggest that all samples are ~ 3.7 nm (~ $2.7 \times 10^{16}$ Ru atoms/cm$^2$) thicker than the nominal value, which is however not the case, since the uncertainty on the measured Ru area density is less than 3%. The offset is not caused by the 0.3 nm of TiN, since the resistivity is much larger than that of Ru, and due to exposure to air before deposition of Ru the TiN is oxidized and thus has an even higher resistivity; as a result TiN contributes negligibly to the transport. In other metal systems, such as Cu,[18] the Hall coefficient has been shown to depend on thickness and this was ascribed to band structure effects. However, in the case of Ru, we suggest that the offset can be explained by the fact that Ru is a compensated metal with an equal number of holes and electrons contributing to the transport and with much higher hole mobility ($\mu_p$) than electron mobility ($\mu_n$).[19] A detailed analysis shows that use of Eq. 1 then results in $\mu_H = (\mu_p - \mu_n)$ and $N_{HS} = P(\mu_p + \mu_n)/(\mu_p - \mu_n)$ if transport and Hall mobilities are identical; here $P$ is the hole sheet density. As a result the calculated Hall sheet carrier density overestimates the real sheet carrier density by the factor $(\mu_p + \mu_n)/(\mu_p - \mu_n)$. This factor is expected to increase as the film thickness decreases, due to a longer mean free path for holes than for electrons, which makes the hole mobility more sensitive to film thickness than the electron mobility. The sheet density measured at thicker films is consistent with approximately one hole per Ru atom, i.e., a hole concentration of $p \simeq 7.4 \times 10^{22}$ cm$^{-3}$, which is 2.6 times higher than that calculated from the bulk Hall coefficient reported by Hurd[20] but in better agreement with the thin film measurements of Steeves.[19]

In Fig. 3(c) the relative standard deviations of $N_{HS}$ and $\mu_H$ are plotted as function of sample thickness. From this plot it is observed that using sub-probe 1347 (non-equidistant) results in relative standard deviations that are 2-4 times lower than those obtained using sub-probe 1357 (equidistant).

From Fig. 3(c) it is also observed that the relative standard deviations are similar to those calculated in Fig. 2. This means the models can potentially be used to design a future probe, such that the influence of position errors and electrical noise are minimized.

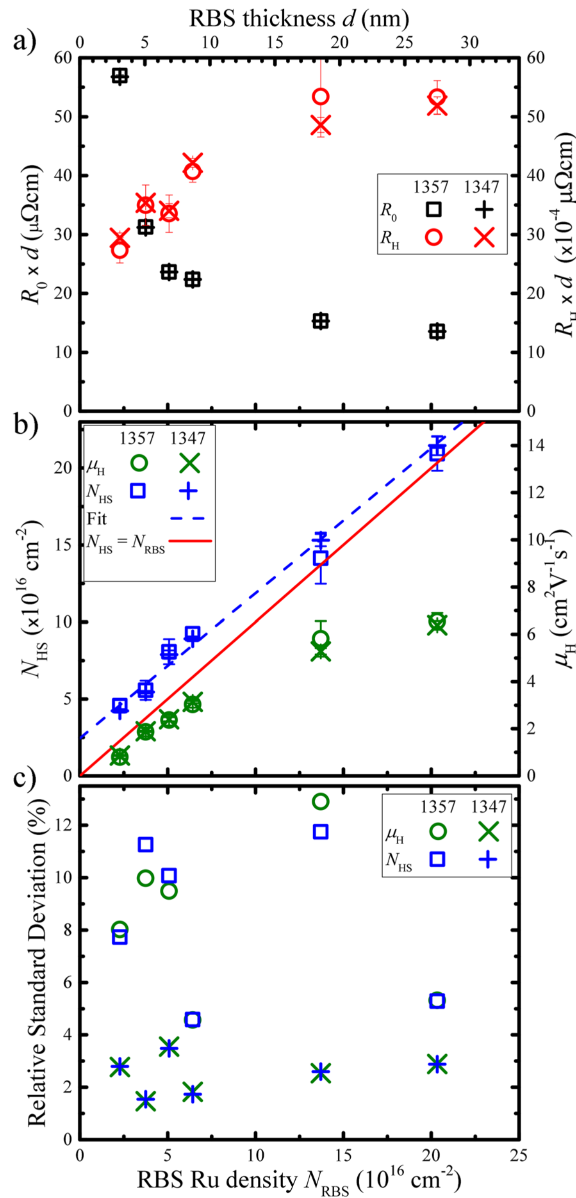


FIG. 3. a) Sheet resistance and Hall sheet resistance multiplied with sample thickness as function of Ru thickness. The error bars correspond to one standard deviation. Note, error bars for the sheet resistance are so short that the points cover them. b) Hall sheet carrier density and Hall mobility as function of Ru thickness. The error bars correspond to one standard deviation. The blue dashed line is a linear fit to the Hall sheet carrier density data while the red line represents the 1:1 correlation. c) Relative standard deviation as function of Ru thickness for Hall sheet carrier density and Hall mobility.

## V. CONCLUSION

In conclusion, we have shown that for samples with $R_0 \gg R_{\mathrm{H}}$, it is possible to reduce the relative standard deviation of Hall sheet carrier density and Hall mobility by changing the inter electrode spacing while keeping the total width of the probe constant. By using four point probes with electrode spacings of 20, 10 and 30 $\mu$m compared to probes with equidistant electrode spacings of 20 $\mu$m, it is possible to reduce the relative standard deviation by a factor of 2-4. Furthermore, an analysis of noise sources is presented, which can be used to design probes that are optimized for measurements on samples with a specific $R_0/R_H$ ratio and a given standard deviation of position error. From measurements on Ruthenium samples ranging in thickness from 3 nm to 30 nm, it is shown

that the Hall sheet carrier density is almost linearly dependent on sample thickness. Thus, the micro Hall effect measurement method can also be used to monitor variations in thickness of thin metal films.

## ACKNOWLEDGMENTS

This work was financially supported by Innovation Fund Denmark grant number 5165-00042B and H2020 European project no. 688225.

[1] D. K. Schroder, *Semiconductor Material and Device Characterization* (John Wiley & Sons, 2006) p. 800.
[2] I. Miccoli, F. Edler, H. Pfnür, and C. Tegenkamp, Journal of Physics: Condensed Matter **27**, 223201 (2015).
[3] C. L. Petersen, F. Grey, I. Shiraki, and S. Hasegawa, Appl. Phys. Lett. **77**, 3782 (2000).
[4] C. L. Petersen, T. Hansen, P. Bøggild, A. Boisen, O. Hansen, T. Hassenkam, and F. Grey, Sensors and Actuators A: Physical **96**, 53 (2002).
[5] D. H. Petersen, O. Hansen, T. M. Hansen, P. Bøggild, R. Lin, D. Kjær, P. F. Nielsen, T. Clarysse, W. Vandervorst, E. Rosseel, N. S. Bennett, and N. E. B. Cowern, Journal of Vacuum Science & Technology B **28**, C1C27 (2010).
[6] F. Werner, Journal of Applied Physics **122**, 135306 (2017).
[7] D. H. Petersen, O. Hansen, R. Lin, and P. F. Nielsen, J. Appl. Phys. **104**, 013710 (2008).
[8] E. Perkins, L. Barreto, J. Wells, and P. Hofmann, Review of Scientific Instruments **84**, 033901 (2013).
[9] S. B. Kjeldby, O. M. Evenstad, S. P. Cooil, and J. W. Wells, Journal of Physics: Condensed Matter **29**, 394008 (2017).
[10] A. Cagliani, D. Kjær, F. W. Østerberg, O. Hansen, P. F. Nielsen, and D. H. Petersen, Measurement Science and Technology **28**, 025012 (2017).
[11] D. H. Petersen, O. Hansen, R. Lin, P. F. Nielsen, T. Clarysse, J. Goossens, E. Rosseel, and W. Vandervorst, in *2008 16th IEEE International Conference on Advanced Thermal Processing of Semiconductors* (2008) pp. 251–256.
[12] F. W. Østerberg, D. H. Petersen, P. F. Nielsen, E. Rosseel, W. Vandervorst, and O. Hansen, J. Appl. Phys. **110**, 033707 (2011).
[13] H. H. Henrichsen, O. Hansen, D. Kjaer, P. F. Nielsen, F. Wang, and D. H. Petersen, in *2014 International Workshop on Junction Technology (IWJT)* (2014) pp. 1–4.
[14] D. Kjaer, O. Hansen, F. W. Østerberg, H. H. Henrichsen, C. Markvardsen, P. F. Nielsen, and D. H. Petersen, Measurement Science and Technology **26**, 095005 (2015).
[15] L. G. Wen, P. Roussel, O. V. Pedreira, B. Briggs, B. Groven, S. Dutta, M. I. Popovici, N. Heylen, I. Ciofi, K. Vanstreels, F. W. Østerberg, O. Hansen, D. H. Petersen, K. Opsomer, C. Detavernie, C. J. Wilson, S. V. Elshocht, K. Croes, J. Bömmels, Z. Tőkei, and C. Adelmann, ACS Applied Materials & Interfaces **8**, 26119 (2016).
[16] M. Popovici, B. Groven, K. Marcoen, Q. M. Phung, S. Dutta, J. Swerts, J. Meersschaut, J. A. van den Berg, A. Franquet, A. Moussa, K. Vanstreels, P. Lagrain, H. Bender, M. Jurczak, S. Van Elshocht, A. Delabie, and C. Adelmann, Chemistry of Materials **29**, 4654 (2017).
[17] J. Meersschaut and W. Vandervorst, Nuclear Instruments and Methods in Physics Research Section B: Beam Interactions with Materials and Atoms **406**, 25 (2017).
[18] J. Gogl, J. Vancea, and H. Hoffmann, Journal of Physics: Condensed Matter **2**, 1795 (1990).
[19] M. M. Steeves, D. Deniz, and R. J. Lad, Applied Physics Letters **96**, 142103 (2010).
[20] C. M. Hurd, *The Hall Effect in Metals and Alloys* (Plenum, New York, 1972).